Tuning of structure inversion asymmetry by the δ-doping position in (001)-grown GaAs quantum wells

V. Lechner,[1] L.E. Golub,[2] P. Olbrich,[1] S. Stachel,[1] D. Schuh,[1] W. Wegscheider,[1] V.V. Bel'kov,[1,2] and S.D. Ganichev[1]
[1] *Terahertz Center, University of Regensburg, 93040 Regensburg, Germany and*
[2] *Ioffe Physico-Technical Institute, Russian Academy of Sciences, 194021 St. Petersburg, Russia*

Structure and bulk inversion asymmetry in doped (001)-grown GaAs quantum wells is investigated by applying the magnetic field induced photogalvanic effect. We demonstrate that the structure inversion asymmetry (SIA) can be tailored by variation of the delta-doping layer position. Symmetrically-doped structures exhibit a substantial SIA due to impurity segregation during the growth process. Tuning the SIA by the delta-doping position we grow samples with almost equal degrees of structure and bulk inversion asymmetry.

PACS numbers: 73.21.Fg, 72.25.Fe, 78.67.De, 73.63.Hs

The generation, manipulation and detection of spin polarized electrons in low dimensional semiconductors are at the heart of spintronics, see e.g. Refs. 1,2,3. A versatile tool to achieve these goals provides spin-orbit coupling which in quantum wells (QWs) based on III-V semiconductors removes the spin degeneracy of the energy bands. The spin-splitting allows one to control the spin polarization by the electric field, determines the spin relaxation rate and can be utilized for all-electric spin injection. The lifting of the spin degeneracy is caused by spin-orbit interaction described by linear in electron wavevector $\boldsymbol{k}$ terms in the effective Hamiltonian $H_{SO} = \sum \beta_{lm}\sigma_l k_m$, where $\boldsymbol{\beta}$ is a second rank pseudo-tensor and σ_l is the Pauli matrix. The microscopic origin of these terms is the structure inversion asymmetry and bulk inversion asymmetry (BIA) which lead to Rashba and Dresselhaus spin-orbit terms in H_{SO}, respectively.[1,2,3] The strength of the BIA spin-splitting depends on the QW width, temperature, and electron density. SIA stems from the inversion asymmetry of the confining potential. The widely applied method of the variation of the SIA related effects is the application of a gate voltage. Recently we demonstrated that in doped (110)-oriented GaAs QWs the proper choice of the δ-doping layer position permits the growth of structures with controllable SIA.[4]

Here we investigate (001)-grown GaAs QWs and demonstrate that SIA is substantially affected by the segregation during the structure growth. This is in contrast to (110)-oriented QWs where the segregation is suppressed.[4] Our experiments explore the role of segregation and allowed us to determine the growth conditions of structures with predetermined SIA. By that, we prepared the QWs with almost equal Rashba and Dresselhaus spin-splittings. Such structures can be applied for the development of a non-ballistic spin-field effect transistor,[5] creation of persistent spin helix[6] and are characterized by a drastic increase of spin relaxation times.[7]

The method to explore the BIA and SIA degrees is based on the investigation of anisotropy of the magneto-photogalvanic effect (MPGE). The MPGE is a photocurrent generation driven by absorption of radiation in QWs in the presence of a magnetic field.[8] The effect is caused by the lack of a space inversion symmetry, thus the strength and the direction of the photocurrent is determined by the interplay of SIA and BIA. The MPGE current density is given by[8]

$$j_\alpha = \sum_{\beta\mu\nu} \phi_{\alpha\beta\mu\nu}\, B_\beta \,(E_\mu E^*_\nu + E_\nu E^*_\mu)/2\,, \qquad (1)$$

where $\boldsymbol{\phi}$ is a fourth rank pseudo-tensor being symmetric in the indices μ and ν, B_β are components of the magnetic field $\boldsymbol{B}$, and E_μ are the components of the radiation electric field $\boldsymbol{E}$. Excitation of (001)-grown QWs with unpolarized radiation at normal incidence in the presence of an external in-plane magnetic field provides a straight forward method to obtain the relative strengths and sign of SIA and BIA. In this case Eq. (1) reduces to $j_l = \sum_m \gamma_{lm} B_m |\boldsymbol{E}|^2$, where $\boldsymbol{\gamma}$ is a second rank pseudo-tensor. It is seen that both MPGE and the spin-splitting are characterized by the same anisotropy in space because they are described by equivalent second rank pseudo-tensors $\boldsymbol{\gamma}$ and $\boldsymbol{\beta}$ whose irreducible components differ by a scalar factor only.

In analogy to the band spin-splitting the photocurrent can be decomposed into SIA and BIA contributions. In particular for an in-plane magnetic field applied along a cubic axis, e.g. y-direction, we obtain for longitudinal, $j_y \parallel [010]$, and transverse, $j_x \parallel [100]$, photocurrents

$$j_x = \gamma^{\mathrm{SIA}}\, B_y\, |\boldsymbol{E}|^2, \quad j_y = \gamma^{\mathrm{BIA}}\, B_y\, |\boldsymbol{E}|^2\,. \qquad (2)$$

Here γ^{SIA} and γ^{BIA} are components of the tensor $\boldsymbol{\gamma}$ due to SIA and BIA, respectively. Taking the ratio j_x/j_y cancels the scalar factor which contains all microscopic details and yields directly the ratio of SIA to BIA. Moreover separate analysis of photocurrents given by Eq. (2) reveals changes of the strength and the sign of SIA and BIA upon a variation of external parameters.

We investigated (001)-oriented Si-δ-doped n-type GaAs/$Al_{0.3}Ga_{0.7}As$ structures grown by molecular-beam epitaxy at temperatures over 600°C. Temperatures T_δ during the growth of the δ-doping layer and subsequent layers, which control the segregation, mobilities μ and

TABLE I: Parameters of samples. Carrier density n_s (per QW-layer) and mobility μ are given for room temperature.

sample	spacer l, nm	spacer r, nm	$\chi = \frac{l-r}{l+r}$	n_s $10^{11}\,\frac{1}{\mathrm{cm}^2}$	μ $10^3\,\frac{\mathrm{cm}^2}{\mathrm{Vs}}$	T_δ °C
1	20	165	-0.78	1.2	7.2	615
2	45	140	-0.51	1.6	7.7	631
3	70	115	-0.24	1.4	8.0	631
4	92.5	92.5	0	1.4	7.7	631
5LT	92.5	92.5	0	1.0	7.9	490
6	106.5	78.5	0.15	1.4	8.1	626
7	111	74	0.20	1.4	8.1	632
8	125	60	0.35	1.4	7.7	629
9	140	45	0.51	1.4	7.9	630
10	165	20	0.78	1.5	8.0	625

carrier densities n_s measured at room temperature are given in Table I. Figure 1 sketches the conduction band edge together with the corresponding δ-doping position. All QWs have the same width of 15 nm but differ essentially in their doping profile: In all structures besides sample 4 and 5LT, the doping layers are asymmetrically shifted off the barrier center either to the left or to the right. The impurities' Coulomb field yields an asymmetric potential profile inside the QWs. To describe the degree of asymmetry we introduce the parameter $\chi = (l-r)/(l+r)$, where l and r are the spacer layer thicknesses between QW and δ-layers (Fig. 1 and Table I). Samples 4 and 5LT contain a Si-δ-sheet, placed in the middle of each barrier between adjacent QWs. All samples were square shaped with the sample edges of 5 mm length oriented along $[1\bar{1}0]$ and [110] crystallographic axes. In order to measure photocurrents, ohmic contacts were alloyed on the sample corners and in the middle of each sample side allowing to probe the photocurrent in different directions, as displayed in Fig. 2. An external in-plane magnetic field $B = \pm 1$ T is applied along either $x \parallel [100]$ or $y \parallel [010]$.

The MPGE is measured at room temperature by exciting the samples with unpolarized terahertz radiation under normal incidence, as sketched in the inset of Fig. 2b. The pulsed radiation of power $P \approx 5$ kW is obtained applying an optically pumped pulsed NH_3 molecular laser.[9] The wavelength of 280 μm was chosen to cause only free carrier absorption of the radiation. To obtain unpolarized light we used a brass cone of 95 mm length with the angle of about 4° which depolarizes the laser radiation as a result of multiple reflection in the cone.

Irradiating samples with unpolarized radiation we observed a photocurrent signal linearly increasing with rising magnetic field strength and changing the sign upon inversion of the magnetic field direction from $B_+ > 0$ to $B_- < 0$. For convenience in the discussion below we evaluate the data after $J = [J(B_+) - J(B_-)]/2$ which yields solely MPGE contribution. The signal is detected in both

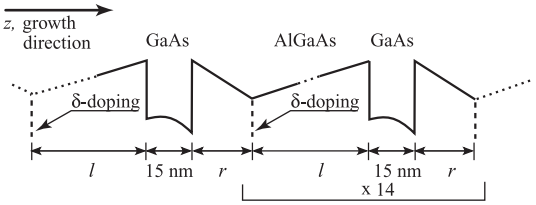

FIG. 1: Band profile of QWs and doping position.

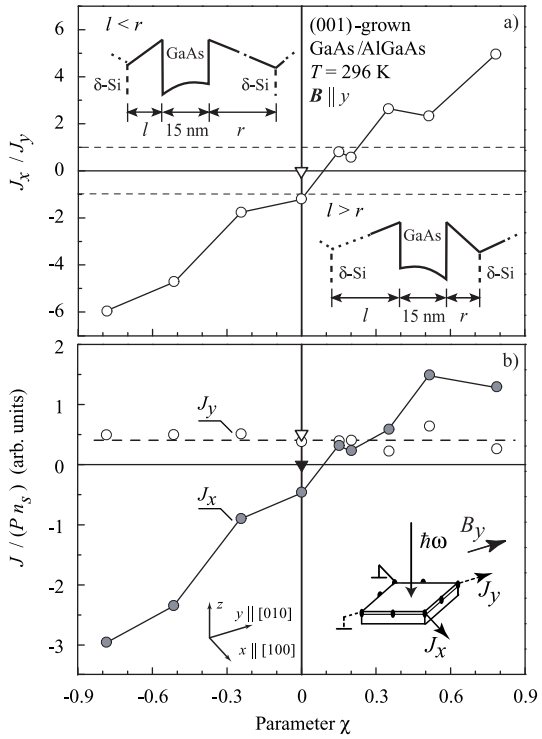

FIG. 2: a) The ratio of the SIA and BIA contributions to the MPGE, J_x/Jy, as a function of χ. Triangle shows the result for sample 5LT grown at $T_\delta = 490$°C, circles demonstrate the data for all other samples grown at $T_\delta \approx 630$°C. Insets show the QW profile and the doping positions for $l < r$ and for $l > r$. b) Dependence J/Pn_s on the parameter χ. The photocurrents are measured along and normal to $\boldsymbol{B}||y$. Full and open symbols show J_x and J_y, respectively (triangles are the data for sample 5LT). Inset shows the experimental geometry.

longitudinal and transverse directions with respect to the magnetic field orientation.

Figure 2a shows the ratio between J_x and J_y photocurrents as a function of the parameter χ obtained for magnetic fields of ± 1 T applied along the y-direction. As addressed above this ratio yields the ratio between SIA and BIA strengths. As an important result Fig. 2a shows that the SIA/BIA-ratio strongly depends on the doping position and, moreover, changes its sign for $\chi \approx 0.1$.

The dependence of the both separate contributions J_x and J_y on the parameter χ is shown in Fig. 2b. Here we normalize the data by the free carrier concentration n_s to enable a comparison of BIA and SIA in different sam-

ples. For the Boltzmann distribution of carriers relevant to experiments at room temperature the MPGE current is proportional to n_s but independent of the electron mobility.[10] Thus, in order to compare the SIA and BIA contributions to MPGE in different samples it is sufficient to normalize the photocurrents by the electron density n_s.

Figure 2b demonstrates that while the longitudinal current is almost independent of χ the transverse current strongly depends on χ. The results of Fig. 2b are in a full agreement with Eq. (2) demonstrating that the longitudinal current in this experimental geometry is solely due to BIA and the transverse current is caused by SIA only. In additional experiments we applied the magnetic field $\boldsymbol{B}$ along the x-direction. We observed that while the data on the transverse current remained the same the longitudinal photocurrent inverted its sign in all samples. This observation is also in agreement with Eq. (1) yielding for $\boldsymbol{B} \parallel x$ that the photocurrent is given by $j_x = -\gamma^{\rm BIA} B_x |\boldsymbol{E}|^2$ and $j_y = \gamma^{\rm SIA} B_x |\boldsymbol{E}|^2$.

The fact that the longitudinal current in both experimental geometries is independent of χ is expected for BIA-induced effects which are obviously insensitive to the magnitude and the sign of χ. The transverse current, in contrast, is caused by SIA and is very sensitive to the impurity potential. The variation of χ affects the degree of asymmetry and even changes the sign of the transverse photocurrent due to SIA for $\chi \approx 0.1$. Our results show that for $\chi < 0.1$ the asymmetry is dominated by the potential of impurities placed on the left (substrate) side of the QW. Figure 2b demonstrates that in order to obtain a vanishing value of SIA (001)-oriented samples must be asymmetrically doped, so that the δ-doping layer on the substrate side is placed at a larger distance than that to the right of the QW ($l > r$). This observation is attributed to the segregation of Si-impurities during the structure growth and is in contrast to (110)-grown structures, where symmetrical doping results in a vanishing SIA.[4] This essential difference stems from the difference in growth conditions. Indeed, the growth temperature of high-quality (001)-oriented QWs is typically higher than 600°C, while (110)-structures are grown at 480°C.[11] The high growth temperature of (001)-oriented heterostructures leads to substantial dopant migration in the growth direction during the growth process (segregation) which affects mostly the substrate side of a QW and results in SIA in symmetrically doped QWs. In order to suppress the segregation we grew a symmetrically doped sample with reduced temperature during the δ-doping ($T_\delta = 490$°C). We find in this case that the MPGE current perpendicular to $\boldsymbol{B}$, which is caused solely by SIA, is almost equal to zero. Thus, our result clearly demonstrates that the reduced growth temperature suppresses segregation, which, therefore, does not introduce additional structure inversion asymmetry.

The next important observation is that for $\chi = 0$ (sample 4) and $\chi \approx 0.17$ (samples 6 and 7) $J_x/J_y \approx \pm 1$ (see Fig. 2a) indicating that SIA and BIA have equal strengths. In such samples the effects due to SIA and BIA, e.g. band spin-splitting, cancel each other in either $[1\bar{1}0]$ or $[110]$ crystallographic directions depending on the relative sign of SIA and BIA terms.[7] For the transverse photocurrent caused by magnetic field applied along one of $\langle 110 \rangle$-axes the phenomenological theory yields $j_\perp = (\gamma^{\rm SIA} \pm \gamma^{\rm BIA}) B |\boldsymbol{E}|^2$, where the two signs correspond to the two magnetic field orientations. At $\gamma^{\rm SIA} \approx \gamma^{\rm BIA}$ one can expect substantial difference in transverse photocurrents at $\boldsymbol{B}$ applied along $[1\bar{1}0]$ and $[110]$. Indeed, this anisotropy was observed: e.g. in sample 4 characterized by close SIA and BIA strengths we found that the transversal signal changes its magnitude by a factor of six under rotation of in-plane magnetic field $\boldsymbol{B}$ by 90 degrees.

To conclude, we investigated SIA and BIA in (001)-oriented GaAs/AlGaAs QWs at room temperature. The observed modulation of the SIA/BIA-ratio by a shift of the doping position demonstrates that the impurity position plays an important role in the SIA. We show that high growth temperatures of high-quality (001)-oriented GaAs QWs add an additional factor to the SIA due to impurity segregation. Our measurements based on the MPGE demonstrate that this method can be successfully applied to study SIA and BIA in QW structures. We emphasize that the method can be applied even at room temperature, where many other methods cannot be used. By investigating samples with a different δ-doping profile we obtained QWs with almost equal magnitudes of Rashba and Dresselhaus constants which should be characterized by extraordinary long spin relaxation times.

This work is supported by the DFG via programs SPP 1285 and SFB 689, RFBR, Russian President grant, and "Dynasty" foundation — ICFPM.

Appendix 1

Polarized light gives rise to new roots of the MPGE due to the optical excitation instead of relaxation which solely determines the photocurrent generated by the unpolarized radiation.[10] We used linearly polarized radiation with the polarization vector of the incoming light rotated applying $\lambda/2$-plate. By that the azimuth angle α is varied between 0° and 180° corresponding to all possible orientations of the electric field vector in the (xy) plane. For linearly polarized radiation at normal incidence and $\boldsymbol{B}$ parallel to x or y axes Eq. (1) takes the form

$$\begin{aligned} j_\parallel &= \pm D_1 B \pm D_3 B \cos 2\alpha + C_2 B \sin 2\alpha, \\ j_\perp &= C_1 B - C_2 B \cos 2\alpha \pm D_2 B \sin 2\alpha, \end{aligned} \qquad (3)$$

where α is the angle between $\boldsymbol{E}$ and $\boldsymbol{B}$, and $\pm$ correspond to $\boldsymbol{B}$ parallel to x and y axes, respectively. The coefficients C_i and D_i are caused by SIA and BIA, respectively. The corresponding contributions to Eq. (3) reflect the different symmetry of SIA and BIA: the SIA induced terms are invariant while the BIA contributions

change their signs under rotation of $\boldsymbol{B}$ and $\boldsymbol{E}$ by 90° around z axis. All photocurrent contributions given by Eq. (3) as well as polarization dependences have been detected in our samples. The photocurrent contributions and the ratio of the corresponding SIA- and BIA-related coefficients behave upon a variation of the parameter χ in agreement with the data obtained using unpolarized radiation. Our results show that in all investigated samples using of polarized radiation does not lead to an increase of the method sensitivity. In some other samples, however, MPGE due to the optical excitation can be substantially larger than that due to relaxation. Therefore the applicability of the method using polarized radiation demonstrated in our experiments may be of importance.

[1] R. Winkler, *Spin-Dependent Transport of Carriers in Semiconductors*, in *Handbook of Magnetism and Advanced Magnetic Materials* (John Wiley & Sons, NY 2007).

[2] J. Fabian et al., Acta Phys. Slov. **57**, 565 (2007).

[3] M. I. Dyakonov, Ed., *Spin Physics in Semiconductors* (Springer, Berlin, 2008).

[4] V. V. Bel'kov et al., Phys. Rev. Lett. **100**, 176806 (2008).

[5] J. Schliemann, J. C. Egues, and D. Loss, Phys. Rev. Lett. **90**, 146801 (2003).

[6] B.A. Bernevig, J. Orenstein, and S.C. Zhang, Phys. Rev. Lett. **97**, 236601 (2006).

[7] N. S. Averkiev and L. E. Golub, Semicond. Sci. Technol. **23**, 114002 (2008).

[8] V. V. Bel'kov and S. D. Ganichev, Semicond. Sci. Technol. **23**, 114003 (2008).

[9] S. D. Ganichev and W. Prettl, *Intense Terahertz Excitation of Semiconductors* (Oxford Univ. Press, Oxford, 2006).

[10] S. D. Ganichev et al., Nature Physics **2**, 609 (2006).

[11] L. Pfeiffer et al., Appl. Phys. Lett. **56**, 1697 (1990).